J|A|C|S
ARTICLES
Published on Web 12/20/2002

Multiple Li Positions inside Oxygen Octahedra in Lithiated TiO_2 Anatase

Marnix Wagemaker,[†] Gordon J. Kearley,[†] Ad A. van Well,[†] Hannu Mutka,[‡] and Fokko M. Mulder*,[†]

Contribution from the Interfaculty Reactor Institute, Delft University of Technology, Mekelweg 15, 2629JB Delft, The Netherlands and Institute Laue-Langevin, BP156, 38042 Grenoble Cedex 09, France

Received August 16, 2002; E-mail: Mulder@iri.tudelft.nl

Abstract: Intercalation of Li in TiO_2 anatase results in a phase separation in a Li-poor and a Li-rich phase. The local lithium configuration in the coexisting crystallographic phases is resolved by detailed analysis of neutron diffraction data. In each of the phases, two distinct positions within the octahedral interstices are found, with a temperature-dependent occupancy. A combination of quasi-elastic neutron scattering and force field molecular dynamics simulations shows that Li is hopping on a picosecond time scale between the two sites in the octahedral interstices. The results also suggest a specific Li arrangement along the crystallographic *a* direction, albeit without long range order. It is likely that multiple discrete Li sites within a distorted oxygen octahedron occur not only in intercalated TiO_2 anatase but also in other (transition metal) oxides.

1. Introduction

The physical and chemical properties of titanium dioxide offer an exciting spectrum of applications having the additional advantage of being biocompatible, environmentally friendly, and readily available. It is used as a white pigment in many products from toothpaste to wall paint. The crystallographic anatase form is of special interest because of its ability to store significant amounts of Li, which finds application as an anode in Li ion (nano)battery materials.[1] The optical properties change upon Li insertion,[2−4] this electrochromic effect being a starting point of displays and smart windows. The semiconductor properties also make it a suitable electrode in the conversion of light energy into electrical energy.[4,5]

In this paper, we focus on the Li ion positions and dynamics of inserted lithium. Schematically the (electro)chemical Li insertion can be written as $TiO_2 + xLi^+ + xe^- \rightarrow Li_xTiO_2$, where x is the mole fraction Li in TiO_2. The maximum Li insertion in TiO_2 anatase varies through the literature from $x = 0.5$ up to 1, depending on the temperature and experimental technique. For chemical intercalation with *n*-butyllithium,[6] which has a potential of 1 V versus Li, $x = 0.6-0.7$ seems to be the most reliable value, while, for electrochemical experiments, $x = 0.5$ is consistently reported as the maximum insertion ratio. The (elastic) interaction force between intercalated Li ions is expected to be attractive[7] and weak Ti−Ti interactions are formed,[8,9] which results in a structural phase transition and separation into a Li-rich and Li-poor phase.[10]

Cava et al.[11] already reported the structure of the lithium-rich phase, here referred to as lithium titanate, and the Li position therein by using neutron diffraction. The structure for composition $Li_{0.5}TiO_2$ was indexed with space group *Imma*, number 74, whereas the space group of the original anatase was already known[12] to be *I*41/*amd*, number 141. The overall orthorhombic distortion of the atomic positions in the change from anatase to lithium titanate is small and leads to more regularly shaped TiO_6 octahedra in lithium titanate than in anatase. The change in symmetry is accompanied by a decrease of the unit cell along the *c* axis and an increase along the *b* axis. According to Cava et al.,[11] the Li ions in the lithium titanate phase are randomly located in about half of the available interstitial octahedral 4e sites, which was also found in theoretical calculations.[13,14]

^{7}Li nuclear magnetic resonance (NMR) results[15] confirmed the two-phase equilibrium between a Li-ion-poor phase with

[†] Delft University of Technology.
[‡] Institute Laue-Langevin.

(1) Huang, S. Y.; Kavan, L.; Exnar, I.; Grätzel, M. *J. Electrochem. Soc.* **1995**, *142*, L142.
(2) Bechinger, C.; Ferrere, S.; Zaban, A.; Sprague, J.; Gregg, B. A. *Nature* **1996**, *383*, 608−610.
(3) van de Krol, R.; Goossens, A.; Meulenkamp, E. A. *Appl. Phys.* **2001**, *90*, 2335.
(4) O'Regan, B.; Grätzel, M. *Nature* **1991**, *353*, 737−740.
(5) Hagfeldt, A.; Grätzel, M. *Chem. Rev.* **1995**, *95*, 49−68.
(6) Wittingham, M. S.; Dines, M. B. *J. Electrochem. Soc.* **1977**, *124*, 1387−1388.
(7) Zachau-Christiansen, B.; West, K.; Jacobsen, T.; Atlung, S. *Solid State Ionics* **1988**, *28−30*, 1176−1182.
(8) Nuspl, G.; Yoshizawa, K.; Yamabe, T. *J. Mater. Chem.* **1997**, *7*, 2529−2536.
(9) Benco, L.; Barras, J. L.; Daul, C. A. *Inorg. Chem.* **1999**, *38*, 20−28.
(10) van de Krol, R.; Goossens, A.; Meulenkamp, E. A. *J. Electrochme. Soc.* **1999**, *146*, 3150−3154.
(11) Cava, R. J.; Murphy, D. W.; Zahurak, S.; Santoro, A.; Roth, R. S. *J. Solid State Chem.* **1984**, *53*, 64−75.
(12) Murphy, D. W.; Greenblatt, M.; Zahurak, S. M.; Cava, R. J.; Waszczak, J. V.; Hull, G. W.; Hutton, R. S. *Rev. Chim. Miner.* **1982**, *19*, 441−449.
(13) Lunell, S.; Stashans, A.; Ojamae, L.; Lindstrom, H.; Hagfeldt, A. *J. Am. Chem. Soc.* **1997,** *119*, 7374−7380.
(14) Stashans, A.; Lunell, S.; Bergström, R.; Hagfeldt, A.; Lindquist, S. E. *Phys. Rev. B* **1996**, *53*, 159−170.
(15) Wagemaker, M.; van de Krol, R.; Kentgens, A. P. M.; van Well, A. A.; Mulder, F. M. *J. Am. Chem. Soc.* **2001**, *123*, 11454−11461.

10.1021/ja028165q CCC: $25.00

the original anatase structure (here referred to as lithiated anatase) and the Li-ion-rich lithium titanate structure for overall compositions $x = 0.07-0.6$. The Li position in the original anatase structure is unknown and can most likely only be found by a careful neutron diffraction study because of the small Li fraction Li/Ti ≈ 0.01, as was determined by NMR.[15] Furthermore, recent ^{7}Li NMR experiments[15,16] which probe the local environment suggested that Li in the lithium titanate structure might not simply occupy one well-defined position in the TiO_2 lattice. This notion was based on the unexpectedly large homogeneous NMR line width of the ^{7}Li in lithium titanate, which might be related to Li residing in one site for a finite time $\approx$ 1/line width and then moving to another site with another NMR spectrum. So far, neutron diffraction has not been applied to determine the Li ion positions in compositions Li/Ti > 0.5. This is especially relevant because of a new Li NMR resonance that was observed[17,15] for Li/Ti $\geq$ 0.5 with an even larger line width than that in lithium titanate $Li_{0.5}TiO_2$. Although Luca et al.[17] suggested this new Li environment to be weakly coupled with conduction electrons, a new structural environment for lithium in lithium titanate for Li/Ti $\geq$ 0.5 can be also considered.

In this paper, the detailed Li position(s) and dynamics within the oxygen octahedra are studied in both coexisting phases: lithiated anatase and lithium titanate as well as in $Li_{0.6}TiO_2$. The paper has two parts. In the first part, neutron diffraction is applied as a function of temperature and composition to determine the Li ion positions and the overall structure. Neutrons are preferred over X-rays, because of the sensitivity of neutrons for Li and the large region in reciprocal space that can be probed with neutrons (as many diffraction peaks as possible are required). In the second part, the local Li ion dynamics is probed by temperature-dependent quasi-elastic neutron scattering (QENS) in comparison with molecular dynamics simulations based on the COMPASS force field.[18]

2. Experimental Section

Sample Preparation. Microcrystalline TiO_2 (anatase) (99%, particle size 2−20 μm) was obtained from Janssen Chemica. Li_xTiO_2 samples were prepared by chemical intercalation of the TiO_2 powder with *n*-butyllithium[6] (1.6 M Aldrich). Four Li_xTiO_2 samples were prepared with overall compositions $x = 0.12$, 0.35, 0.5, and 0.6. All sample preparations were carried out in an argon atmosphere glovebox to prevent reaction of Li with air and moisture. After preparation, the samples were subjected to wet-chemical inductively coupled plasma spectroscopy (ICP) analysis (approximately 5% accuracy) to check the overall composition (ratio Li/Ti). These results confirmed that during preparation all the lithium reacted with the TiO_2 (anatase), thus yielding the overall compositions described. The exception is $x = 0.6$, where ICP indicated a maximum Li content of $x \approx 0.6$, irrespective of the surplus of *n*-butyllithium.

Neutron Diffraction. Because subtle changes both in structure and in Li position(s) and site occupation(s) are expected; both high intensity and resolution in *d* spacing are necessary. Although neutrons are very sensitive to Li compared with X-rays, the coherent cross section of Li is smaller than that of oxygen and titanium. To meet these high demands, the neutron diffraction experiments were performed at GEM, the high-intensity general purpose time-of-flight diffractometer at the ISIS pulsed neutron source[19] (Rutherford Appleton Laboratory, U.K.). GEM is equipped with more than 5000 detectors in 7 banks covering angles between approximately 159° (backscattering) and 18° (forward scattering). For the present samples, significant intensity was obtained in the *d* spacing range [0.2−8 Å]. All sample compositions ($x = 0$, 0.12, 0.35, 0.5, and 0.6) were measured at 10 and 298 K, but composition $x = 0.35$ was also measured at $T = 20$, 40, 70, and 110 K. Cylindrical vanadium airtight sample cans were used for all the measurements, and stable temperatures between 10 and 298 K were achieved using a helium cryostat. Data were corrected for the scattering of the vanadium and the cryostat with the Ariel software,[20] and Rietveld refinement was performed using GSAS.[21] Besides the atomic and lattice parameters, the absorption, a line broadening parameter, the crystal phase fractions, and background were also fitted. All the refinements resulted in residuals R_p and R_{wp} between 3 and 4%. To determine the Li ion positions, the (differences between) observed and calculated structure factors were obtained with GSAS[21] (Pawley method). Fourier density (difference) maps were obtained from the structure factors using the Fourier formalism implemented in the GFour package.[22] The Li ion positions found were used as input for the Rietveld refinement, resulting in the fits described previously.

Quasi-Elastic Neutron Scattering. A 2 mm thickness of pure lithium titanate sample, $Li_{0.6}TiO_2$, was loaded in a flat plate aluminum sample chamber, under argon atmosphere, and sealed with indium. The quasi-elastic neutron experiments were performed on IN6, a time focusing time-of-flight spectrometer, at the Institute Laue-Langevin (Grenoble, France). For our experiments, $\lambda = 5.12$ Å was chosen, resulting in an energy resolution of 100 μeV. The neutrons are detected by 337 elliptical ^{3}He detectors covering an angular range of $10° < 2\theta < 114°$. This results in a momentum transfer range of about 0.3−2 Å^{-1}. The experiments were performed at 2, 100, 150, and 250 K. The data were corrected for time independent background and the sample container scattering. The relative detector efficiency was determined from vanadium reference spectra. Data were corrected using standard algorithms.

Force Field Molecular Dynamics Simulations. In force field methods, there is the assumption that the system of atoms can be described in terms of classical mechanics. In certain circumstances, force field methods are a good alternative for the more realistic quantum mechanical methods which are computationally more expensive. The force field employed is the COMPASS module[18] in the CERIUS suite.[23] This ab initio force field has been parametrized and validated using condensed-phase properties in addition to various ab initio and empirical data for molecules in isolation and recently also for inorganic materials. It enables accurate and simultaneous predictions of structural, conformational, vibrational, and thermo-physical properties. The models were geometrically relaxed, using the same COMPASS force field (this included the cell parameters). For the interaction between atoms, a semi-ionic model was used, in which, for nonbonding atoms, the interaction energy is represented by an electrostatic term and the Lennard−Jones function and, for bonding atoms, a Morse dispersion function in addition to the electrostatic term. For the MD simulations, a typical time step size of 1.0×10^{-15} s was chosen;[24] longer step sizes normally lead to unreliable calculations. Our calculation extended to 1.0×10^{-9} s for models up to $3 \times 3 \times 2$ ($a \times b \times c$) unit cells of lithiated TiO_2 anatase. For the static potential calculation, the Li ion trajectory was divided into 20 positions. At each position, the geometry was optimized, using the same force field.

(16) Wagemaker, M.; Kentgens, A. P. M.; Mulder, F. M. *Nature* **2002**, *418*, 397−399.
(17) Luca, V.; Hanley, T. L.; Roberts, N. K.; Howe, R. F. *Chem. Mater.* **1999**, *11*, 2089−2102.
(18) Sun, H. *J. Phys. Chem.* **1998**, *102*, 7338.
(19) Williams, W. G.; Ibberson, R. M.; Enderby, P. D. *Physica B* **1998**, *241−243*, 234−236.
(20) Radaelli, P.G. http://www.isis.rl.ac.uk/disordered/GEM/Software/Ariel3.1release.htm.
(21) Larson, A. C.; Dreele, R. B. V. *GSAS*; Technical Report NM87545; Los Alamos National Laboratory: Los Alamos, NM, 1994.
(22) Gonzalez-Platas, J.; Rodriguez-Carvajal, J. ftp://charybde.saclay.cea.fr/pub/divers/fullprof.2k/Windows/.
(23) Delley, B. *J. Chem. Phys.* **1990**, *92*, 508.
(24) Leach, R. L. *Molecular Modelling*; Pearson Education Limited: Harlow, U.K., 2001.

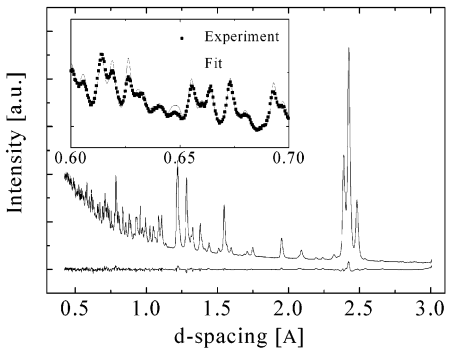

Figure 1. Neutron diffraction ($2\theta = 91.38°$) pattern for $Li_{0.35}TiO_2$ including fit (dotted line in the inset) and fit residual. In the inset, a segment of the pattern at small *d* spacing illustrates the large number of resolved diffraction peaks.

3. Structure of Li_xTiO_2 Anatase

Diffraction. In Figure 1, a typical neutron diffraction spectrum is illustrated. The reflections observed, for all compositions and temperatures, are in agreement with the space groups with which the two phases were previously indexed, *I*41/*amd* (number 141) for lithiated anatase and *Imma* (number 74) for lithium titanate. Where appropriate, the diffraction patterns were refined with a combination of the two phases. In Figure 1, the difference between fitted and observed intensities is shown, indicating the very good fit quality; similar fit quality was found for all refined patterns.

Two-Phase Morphology. Progressive insertion of lithium in TiO_2 anatase leads to an increase of the lithium titanate phase fraction and a decrease of the lithium anatase phase fraction. In agreement with the XRD and NMR results presented in a previous publication,[15] only the ratio between the phases changes as more lithium is inserted. As a function of temperature ($T = 10-298$ K), the ratio between the two phases does not change significantly. The observed line broadening of the powder reflections is a clear indication of domain sizes of the two phases, the domain sizes being significantly smaller than the initial TiO_2 powder particles. The Li-rich lithium titanate and Li-poor lithium anatase phases coexist within one TiO_2 micron-sized particle.[15,16] As the overall lithium content increases, the Li-rich lithium titanate phase domains grow, whereas the Li-poor phase domains become smaller.

Li Ion Positions. To find the Li positions in both phases, the structure factors from both the observed and calculated patterns were extracted. The model for the calculated structure factors contained the optimized Ti and O parameters but did not include the unknown Li position(s). In this way, the Fourier transform of the difference between the observed and calculated structure factors indicates the Li position(s) within the lattice. The obvious way to confirm, and to further quantify, the Li position(s) found in the density-difference plot is to use the resulting position(s) as initial values in further refinement.

The density-difference plot for lithium anatase at 10 K in Figure 2 is extracted from the diffraction pattern taken from the sample with the largest fraction of lithium anatase, composition $Li_{0.12}TiO_2$. Because of the expected small Li fraction in anatase, approximately[15] 0.01, the measurement time for this composition was about 10 times longer than the times for the other measurements. In Figure 2, the oxygen and titanium positions are indicated and the two small spots between the

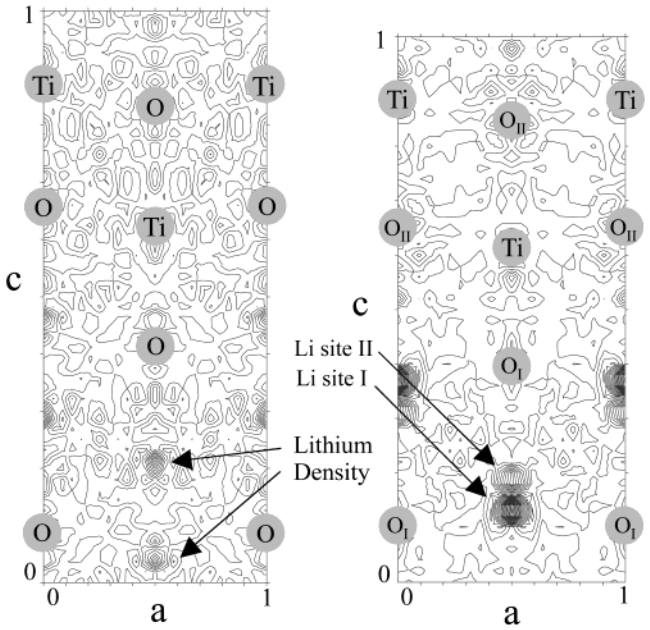

Figure 2. (Left) Fourier scattering length density-difference plot of the lithium anatase phase in the $Li_{0.12}TiO_2$ sample indicating possible Li positions at 10 K. (Right) Fourier scattering length density-difference plot of the lithium titanate phase in the $Li_{0.5}TiO_2$ sample indicating possible Li positions at 10 K. For both plots, the density is a section of the unit cell at $y = 0.25b$.

oxygens represent the intensity that is missing in the model because it does not contain the Li atoms. This indicates that the Li has two possible positions in the oxygen octahedra. Given the small distance between the two sites, 1.61 Å, it is unreasonable that the two positions are occupied simultaneously within one oxygen octahedron because of the repulsive Coulomb interactions between the Li ions. The density-difference plot thus represents an average occupation over all the unit cells. To verify the Li density in Figure 2, which can be represented by a single crystallographic position in the tetragonal *I*41/*amd* space group, they were included in the Rietveld refinement. Although the Li fraction is very small, the refinement was stable and the fit residue was slightly, but significantly, reduced upon adding the two Li positions (from $R_p = 3.38$, $R_{wp} = 4.34$ to $R_p = 3.06$, $R_{wp} = 4.12$ at 10 K). The fit results are included in Table 1. For comparison, the fitted parameters of pure anatase are also listed in Table 1. The Li/Ti ratio is about 0.026, which is larger, but of the same order as 0.01, found with quantitative NMR experiments.[15] Comparison of the unit cell dimensions of pure anatase and the $Li_{x\approx0.01}TiO_2$ (Table 1) phase suggests that even the small Li ion fraction causes a subtle distortion of the anatase lattice: *a* and *b* increase, whereas *c* decreases. This is similar, though rather less, than the distortion of the lithium-rich lithium titanate phase (see later). Unfortunately, because of the small lithium fraction, it was not possible to derive composition and temperature-dependent parameters.

The density-difference plot of the lithium titanate phase resulting from the $Li_{0.5}TiO_2$ sample at 10 K in Figure 2 indicates two possible Li positions very close to each other compared with Li in lithium anatase in the same figure. Again, Rietveld refinements confirm the two positions found in the density-difference plots, the results of which are collected for $T = 10$ K in Table 2. Also in lithium titanate, Li does not occupy more than one position within one oxygen octahedron because of

Table 1. Unit Cell Parameters and Atom Positions of Anatase, Lithium Anatase (Sample $Li_{0.12}TiO_2$; Fit Residue, $R_p = 3.06$, $R_{wp} = 4.12$), Lithium Titanate (Sample $Li_{0.5}TiO_2$; Fit Residue, $R_p = 3.32$, $R_{wp} = 4.21$), and $Li_{0.6}TiO_2$ (Fit Residue, $R_p = 3.40$, $R_{wp} = 4.33$) at 10 K

	Wykoff symbol	*x*,*y*,*z* coordinates [0–1]*a*,*b*,*c*	fraction [0–1]
	TiO_2 anatase (*I*41/*amd*[a])		
Ti	4a	0,0.75,0.1250	1
O	8e	0,0.75,0.3333	1
lattice parameters	$a = 3.7867$		
	$b = 3.7867$		
	$c = 9.5149$		
	lithium anatase (*I*41/*amd*[a])		
Ti	4a	0,0.75,0.1250	1
O	8e	0,0.75,0.3334	1
Li	8e	0,0.75,0.5401	0.013
lattice parameters	$a = 3.7919$		
	$b = 3.7919$		
	$c = 9.4973$		
	lithium titanate (*Imma*)		
Ti	4e	0,0.25,0.8871	1
O_I	4e	0,0.25,0.1037	1
O_{II}	4e	0,0.25,0.6518	1
Li_I	4e	0,0.25,0.3651	0.32
Li_{II}	4e	0,0.25,0.2881	0.19
lattice parameters	$a = 3.8186$		
	$b = 4.0842$		
	$c = 9.0656$		
	$Li_{0.6}TiO_2$ (*Imma*)		
Ti	4e	0,0.25,0.8869	1
O_I	4e	0,0.25,0.1041	1
O_{II}	4e	0,0.25,0.6525	1
Li_I	4e	0,0.25,0.3569	0.38
Li_{II}	4e	0,0.25,0.2888	0.21
lattice parameters	$a = 3.8141$		
	$b = 4.0771$		
	$c = 9.042$		

[a] Origin choice 2.

Table 2. Interatomic Distances (Å) and Their Number (in Parentheses) in the Structures TiO_2 Anatase (*I*41/*amd*, rt), Lithium Anatase (*I*41/*amd*, 10 K), Lithium Titanate (*Imma*, 10 K), and $Li_{0.6}TiO_2$ (*Imma*, 10 K)

structure[a]	lithium anatase	lithium titanate	$Li_{0.6}TiO_2$
Ti−Ti	3.0384 (4)	3.1344 (2)	3.1252 (2)
Ti−Ti		2.8914 (2)	2.8878 (2)
$Ti-O_{eq}$	1.9367 (4)	1.9416 (2)	1.9400 (2)
$Ti-O_{eq}$		2.0438 (2)	2.0402 (2)
$Ti-O_{ax}$	1.9792 (2)	1.9639 (1)	1.9641 (2)
$Ti-O_{ax}$		2.1331 (1)	2.1196 (2)
Li_I-O_{eq}	1.9400 (2)	2.0487 (2)	2.0403 (2)
Li_I-O_{eq}	2.2445 (2)	1.9301 (2)	1.9394 (2)
Li_I-O_{ax}	1.9631 (1)	2.3697 (1)	2.2860 (1)
Li_I-O_{ax}	3.5757 (1)	2.5991 (1)	2.6730 (1)
$Li_{II}-O_{eq}$		2.1135 (2)	2.1389 (2)
$Li_{II}-O_{eq}$		2.1465 (2)	2.1065 (2)
$Li_{II}-O_{ax}$		1.6717 (1)	1.6702 (1)
$Li_{II}-O_{ax}$		3.2972 (1)	3.2888 (1)
$Li_{av}-Li_{av}$	3.0383 (4)	2.5473 (2)	2.5428 (2)
$Li_{av}-Li_{av}$		3.5033 (2)	3.4954 (2)

[a] Subscripts eq and ax denote the oxygen coordination in the *xy* plane and in *c* direction, respectively. Li_{av} refers to the average position of Li in the oxygen octahedron, which is located approximately midway between site I and II.

repulsive Coulomb interactions between the Li ions. The difference in densities between the two Li sites in Figure 2 illustrates that the two Li positions are not occupied evenly on average over the crystal. The positions are not symmetrically

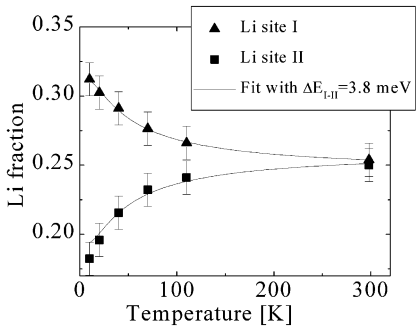

Figure 3. Lithium fraction resulting from refinement from both Li sites in the lithium titanate phase ($Li_{0.52}TiO_2$) as a function of temperature (overall sample composition $Li_{0.35}TiO_2$). The line is a best fit with a Boltzmann distribution of Li over the sites.

equivalent as in lithium anatase and were fitted separately, the fit results being presented in Table 1.

The discrepancy between the present results and the neutron diffraction results of Cava et al.[11] is subtle and concerns the occurrence of the two lithium positions in lithium titanate. The Ti and O positions are identical, within the experimental accuracy. Cava et al. found one Li ion site, *z* coordinate 0.343*c*, located between the two sites found in the present work. When only one possible position is assumed, refinement of our data results in the same Li position found by Cava et al. In particular, at room temperature a good fit with one Li ion position is obtained, but with a substantial anisotropic temperature factor in the *c* direction. However, the two positions found with the density-difference analysis improved the fit quality significantly (from $R_p = 3.71$, $R_{wp} = 4.92$ to $R_p = 3.32$, $R_{wp} = 4.21$ at 10 K), even at room temperature (from $R_p = 3.96$, $R_{wp} = 4.77$ to $R_p = 3.67$, $R_{wp} = 4.52$ at rt), and thus gives a better description of the system. Further, this is in agreement with our dynamical measurements and MD simulations.

The composition of lithium titanate $x \approx 0.5$ might suggest a possible ordering of Li or/and $Ti^{3+}-Ti^{4+}$, as already proposed by Murphy et al.[12] If such an ordering implies a multiple unit cell, one expects super structure reflections corresponding to the larger unit cell. Such ordering can be rejected, since no extra peaks were observed at high *d* spacings in any of the spectra. Ordering within the lithium titanate *Imma* unit cell would lead to a reduction in symmetry, as the Li and/or Ti positions (all equivalent in *Imma*) will become nonequivalent (*Imm*2 space group). Our results corroborate those of Cava et al. in that the present results do not indicate such an ordering because the fit quality did not improve significantly within the *Imm*2 space group.

The considerable Li fraction in lithium titanate enables the study of the Li fractional site occupation as a function of temperature and composition. The Li fraction versus temperature of both Li sites, I and II, is shown in Figure 3. The fact that the Li fractions become equal at high temperatures, whereas they were different at lower temperatures, can be interpreted as the result of a difference in energies between Li residing in site I and in site II, hence a preference for Li to reside at I. Fitting the site occupancy assuming a Boltzmann distribution, as shown in Figure 3, indicates that the energy of a lithium ion is 3.8 meV lower in site I compared with site II. The distance between site I and II in the *c* direction becomes marginally smaller with increasing temperature. The total Li/Ti fraction in lithium titanate

is about 0.52 averaged over all temperatures and is constant with temperature. This is in agreement with the value suggested by the quantitative NMR results[15] ($x = 0.5-0.6$). These results for lithium titanate were derived for a sample with overall composition $Li_{0.5}TiO_2$ (result ICP analysis). Part of this sample has the lithium anatase structure (phase fraction lithium anatase, 0.0908; lithium titanate, 0.9092). The overall composition resulting from the fitted fractions is $Li_{0.48}TiO_2$, in good agreement with the fraction resulting from ICP analysis.

The Li concentration in the lithium titanate phase can be increased up to ~0.6 Li/Ti in case of chemical lithiation with butyllithium. With ^{7}Li NMR, a second Li environment in the lithium titanate structure was observed.[15,17] Density-difference analysis and subsequent Rietveld refinement resulted in the same two Li positions and a slightly distorted structure compared with the original lithium titanate. The refined parameters are listed in Table 1. Therefore, the new ^{7}Li NMR resonance that appears for lithium insertion fraction Li/Ti $\geq$ 0.5 cannot be explained by an additional Li ion structural environment, which, in addition to the arguments of Luca et al.,[17] indicates an electronic origin of the additional Li ion environment in compositions with Li/Ti $\geq$ 0.5. Also, in $Li_{0.6}TiO_2$, there is no indication for nonequivalent Li_I, Li_{II}, or Ti atoms within the *Imma* unit cell or ordering leading to a superstructure. The refined Li fraction is comparable to what is expected on the basis of the ICP results: it increased from 0.52 in lithium titanate to 0.59 in $Li_{0.6}TiO_2$.

The changes of unit cell dimensions of the anatase structure upon lithiation toward lithium titanate are in agreement with those reported previously.[11] The unit cell volume increases by about 3%. In lithium titanate, the *a* and *b* axes become different in length by about 7%, mainly increasing in the *b* direction, and the unit cell decreases by about 5% in the *c* direction (cf. Table 1). Upon intercalation, the Li electron density fills the states at the bottom of the conduction band that are Ti−O antibonding and Ti−Ti bonding.[9] As a consequence, the structure is deformed in such a way that Ti−O distances are elongated and Ti−Ti distances are shortened (conform data in Table 2). Occupation of these bonding bands causes two of the four smallest Ti−Ti distances to decrease upon lithiation and form zigzag chains of Ti atoms in the *b* direction. This causes a reduction in symmetry going from the anatase structure (*I*41/*amd*) to the lithium titanate structure (*Imma*) and the change of the *a* and *b* unit cell lengths in lithium titanate. Increasing the lithium fraction from lithium titanate to $Li_{0.6}TiO_2$ can be expected to lead to a progressive filling of the Ti−Ti $3d_{yz}$ bonding bands, resulting in a very small decrease, from 2.8914 to 2.8878 Å, of these Ti−Ti chain bond lengths.

Two equivalent Li ion positions are found in lithium anatase, symmetrically located with respect to the middle of the oxygen octahedron. In lithium titanate two possible lithium positions are also found within one oxygen octahedron. However, the positions are separated (in the *z* direction) by 0.7 Å compared to 1.61 Å in lithium anatase. This is most likely the result of the deformation of the oxygen octahedron in lithium titanate which becomes smaller in *c* direction with the four equatorial oxygens (near the *ab* plane) more in plane (see Table 2).

Inspection of Figure 4 and of the Li−O distances in lithium anatase and in lithium titanate, Table 2, indicates that lithium in anatase and lithium site II in lithium titanate are effectively

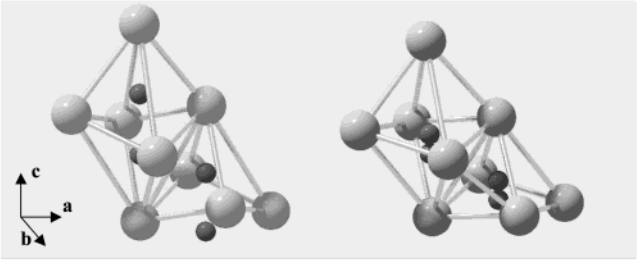

Figure 4. (Left) Two neighboring oxygen octahedra in lithium anatase (spacegroup *I*41/*amd*) with the available Li ion sites. (Right) Two neighboring oxygen octahedra in lithium titanate (spacegroup *Imma*) with the available Li ion sites. In the left (right) octahedron, the top (bottom) Li ion site represents the position referred to as site I.

5-fold coordinated rather than 6-fold coordinated, as suggested by the octahedral coordination. Lithium at site I in lithium titanate is located more toward the center of the oxygen octahedron, and its octahedral oxygen coordination is more regular compared with that of site II.

The relative preference for lithium to reside in site I rather than site II in lithium titanate results from the 3.8 meV energy difference between the sites. This may be due to the distance between two nearest neighboring Li_{II} sites (in the *a* direction) being short compared with Li_I neigboring Li_{II} and with two neighboring Li_I sites. Hence, the latter will suffer less Li−Li coulomb repulsion. This qualitatively explains the difference in occupancy.

Each octahedral interstice has four nearest neighboring interstices which are all at the same distance in the anatase structure but split in two pairs in lithium titanate, the shorter being in the *a* direction. Consequently, the Li−Li distances between Li in one interstice and another (either Li_I-Li_I, Li_I-Li_{II}, or $Li_{II}-Li_{II}$) are smaller in the *a* direction. The average Li−Li interoctahedral distance is $\approx$ 2.5 Å in the *a* direction and $\approx$ 3.5 Å in the *b* direction. As with the Ti−Ti distances, we can consider Li−Li zigzag chains of sites in the *a* direction (the Ti−Ti chains are in the *b* direction). On the basis of the difference between the distances between Li ion sites, we expect that the number of Li neighbors will be minimal on sites in the chain direction because of repulsive Coulomb interactions. This will be less important for the nearest Li neighbor located in sites in another chain. At Li occupation 0.5, one might expect that on average each Li in the octahedral interstice is neighbored in the chain direction by two empty sites to minimize the Coulomb interaction. This proposed site occupation model explains both the preference for the ~0.5 lithium occupation in lithium titanate of the available positions and the difficulty of increasing this because of unfavorable in-chain nearest neighbors. The Li ordering in the chain direction will be obscured by the absence of ordering between the Li ion positions in different chains and hence is unlikely to be observed in diffraction, as is the case in the present results. We anticipate that the dynamic behavior of the lithium ions, hopping between octahedra,[15] will also result in increased disorder.

4. Intraoctahedron Lithium Ion Mobility

To study the Li ion dynamics within the oxygen octahedron in lithium titanate, incoherent quasi-elastic neutron scattering experiments were performed (the Li fraction in lithium anatase is too small to conduct such a study). Quasi-elastic incoherent

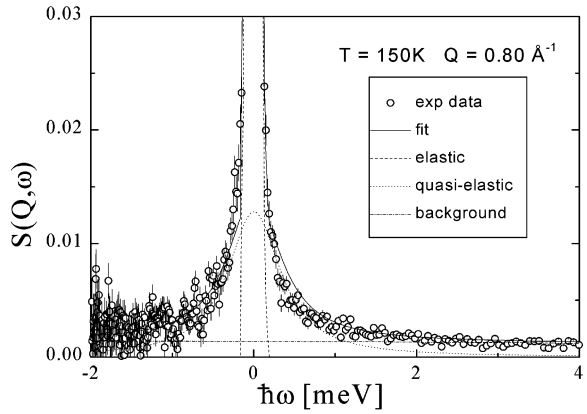

Figure 5. Quasi-elastic neutron spectrum of $Li_{0.6}TiO_2$ at 150 K for momentum transfer $Q = 0.8$ Å. The fitted elastic and quasi-elastic contribution are also shown.

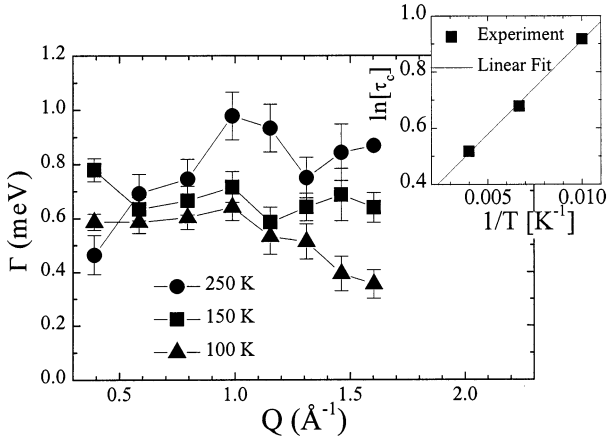

Figure 6. Quasi-elastic line width as a function of momentum transfer for different temperatures. The inset is an Arrhenius plot for the correlation time associated with the quasi-elastic line width (see text).

scattering measures the correlation function for a given particle, in this case Li, to be in a certain volume at a certain time, if it were in that volume at time zero. The energy transfer determines the time scale of the particle dynamics, and the momentum transfer is inversely related to the dimensions in which the motion takes place. The incoherent scattering length of Li is relatively small, compared with that of hydrogen for which many successful quasi-elastic studies have been reported,[25] but TiO_2 as compound has almost negligible incoherent scattering. Consequently, the incoherent signal in Li_xTiO_2 mainly arises from Li. The experimental quasi-elastic neutron scattering results will be compared to molecular dynamics force field simulations of the Li ion movement based on the structural parameters determined by neutron diffraction in the previous section.

Quasi-Elastic Neutron Scattering Results. The neutron scattering spectra were measured at different momentum transfers, Q. An example at one Q value is shown in Figure 5. A fit was made over all Q values using a single Lorentzian function and a δ function centered at zero energy transfer. The resulting functions were convoluted with the measured resolution functions. In Figure 6, the full width at half-maximum $\Gamma(Q)$ (fwhm) of the quasi-elastic component is displayed as a function of Q for different temperatures. For the random diffusion of Li ions, the line width, $\Gamma(Q)$, would increase with[26] Q^2. In contrast,

(25) *Methods Of Experimental Physics 23B*; Academic Press Inc.: London, 1987.

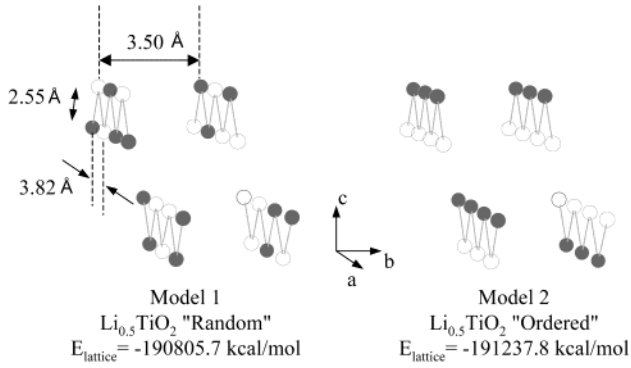

Figure 7. Schematic view of the Li ion octahedral occupations in model 1 and 2; a dark sphere represents an occupied lithium site. For simplicity, the two Li ion sites, Li_I and Li_{II}, are represented as one site.

$\Gamma(Q)$ in the present work is constant with Q and increases with temperature. The QENS experiments therefore indicate a single time scale of Li ion motion that is thermally activated. The Lorentz shaped broadening indicates a relaxation of the self-correlation function of the form $\exp(-t/\tau_c)$, where $\tau_c = 2/\Gamma$ is the correlation time, which for jump processes can be associated with the mean average time Li resides at a certain position. At $T = 2$ K, the line width equals that of the resolution function (100 μeV) corresponding to 13.2 ps; this means $\tau_c > 13.2$ ps. If we assume the time scale of the Li mobility to be thermally activated, the correlation time will obey an Arrhenius law, $\tau_c = \tau_\infty \exp(E_A/k_BT)$, where E_A is the activation energy of the jump process and $1/\tau_\infty$ is the attempt frequency. The results for the data in Figure 6 are $E_A = 5.7 \pm 0.3$ meV (66.7 K) and $\tau_\infty = 1.28 \pm 0.03$ ps.

Molecular Dynamics Simulations. Various models were subject to the MD simulations differing in Li fraction and distribution, a few of which we explicitly report here. In Figure 7, schematic views of model 1 and 2 are presented. In model 1, lithium is initially randomly distributed over half of the octahedral sites (site I or II within the oxygen octahedron). Model 2 represents again lithium titanate where the octahedral interstices in the $-a$ and $+a$ direction (the "chain" direction representing the nearest neighboring Li ion positions) are occupied every second position. Thus, each Li ion is neighbored by unoccupied Li sites in the $-a$ and $+a$ direction and as for model 1, half of the octahedral interstices are occupied by a lithium atom. Li randomly occupies site I or II within the octahedron. This model for the Li-positions ordered in the a direction was proposed in section 3 based on minimizing the repulsive Coulomb interactions between the Li ions. A third model was considered with only one Li atom, which for this model size results in $Li_{0.01}TiO_2$. This resembles Li in anatase rather than Li in lithium titanate. It is interesting to note that although the single Li ion was placed in the titanate lattice, relaxation of the structure including the cell parameters, resulted in the tetragonal anatase structure (the a and b lattice parameters become equal). Before the MD simulations were performed, all models were fully relaxed by minimizing the energy. Comparing the lattice energy (given in Figure 7) between model 1 and 2, for lithium titanate, illustrates what was intuitively argued previously. The absence of nearest Li ion neighbors in the a direction (model 2, referred to as a Li ion ordering in the

(26) Bee, M. *Quasielastic Neutron Scattering*; Adam Hilger: Bristol and Philadelphia, PA, 1988.

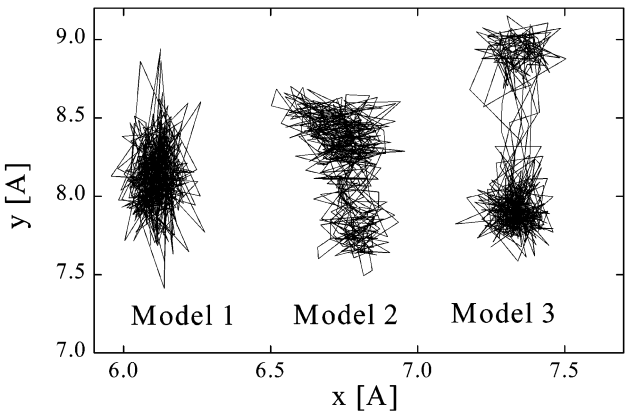

Figure 8. Lithium trajectory, projected on the *ac* plane which intersects with the two lithium sites, calculated with the MD simulations for the different models (see text).

a direction) is energetically favorable compared to a random Li ion occupation of the available sites (model 1) where a number of Li ions have nearest Li ion neighbors in the *a* direction (see section 3).

In Figure 8, the Li trajectory resulting from the molecular dynamics calculation at 250 K is plotted for the different models in the *ac* plane, the same plane as the density-difference plots presented in Figure 2. For model 1, the expected two sites can hardly be recognized in the cigar shaped density. In contrast, in model 2 representing lithium titanate, the two sites I and II are clearly recognized. Vibrations within the site and the hopping between the sites can be distinguished. The distance between the sites is approximately 0.8 Å, in good agreement with the experimental value of 0.7 Å (see section 3).

Model 3 should be compared with the lithium-poor lithium anatase phase. In agreement with the experimental result, the two Li ion positions within the oxygen octahedron are separated by a larger distance compared with lithium in lithium titanate; calculated is 1.5 Å (see Figure 8) and experimental is 1.61 Å (see Table 1).

We wish to compare the time scale of the intraoctahedron hops calculated for lithium titanate with the experimental QENS data. For that, we use the results of model 2 which seems to represent the lithium titanate better than the other presented models. Calculations were performed covering times up to 1 ns. The time scales of the local Li vibrational motion and the intraoctahedron hops are well separated in the lithium mobility power spectrum, Figure 9. During the calculations, the intraoctahedron hops occur at lower frequencies. As a result, the characteristic frequency for this process has a relatively weak signal compared with the local Li vibrations. From the power spectrum, an average jump frequency of the Li ions, equal to the inverse of the correlation or mean residence time for a Li ion to reside at a given site, can be deduced. The correlation time at 250 K is approximately 3 ps (mean value of the envelope) for the intraoctahedron hops.

For lithium in the anatase structure, model 3, the power spectrum (not shown) leads to smaller frequencies for the intraoctahedron hops and in a correlation time of approximately 20 ps. This is not surprising because the two sites in the oxygen octahedron are further apart, and probably separated by a higher potential barrier.

The elastic incoherent structure factor (EISF) can be calculated from the MD trajectories, the results being illustrated in

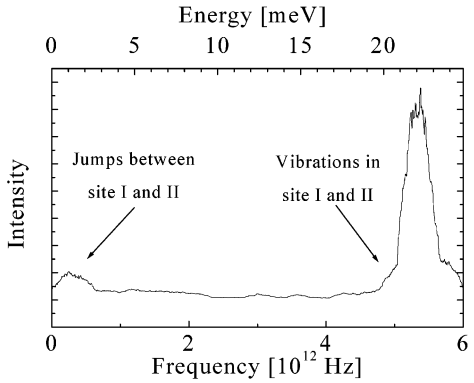

Figure 9. Lithium mobility power spectrum resulting from the MD simulations of model 2 representing lithium in lithium titanate (see text).

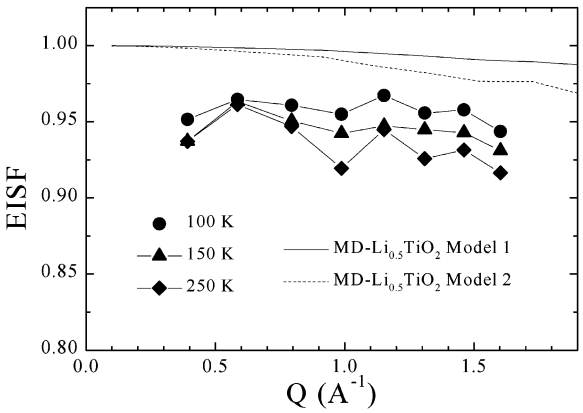

Figure 10. Elastic incoherent structure factor (EISF) as a function of momentum transfer for different temperatures. Also included are calculated EISF curves based on the molecular dynamics calculations presented in text.

Figure 10 for the two models representing lithium titanate. The limited *Q* range of the experiments and the small amplitude of the Li ion dynamics do not allow any discrimination between the different models for the EISF.

Within the best proposed model (model 2), it is interesting to calculate the Li ion potential along the *c* axis, because one would expect to find two minima in energy at the two Li ion sites within the oxygen octahedron. During these (static) calculations, the unit cell dimensions and the position of the Li ion under investigation were fixed, whereas the other atoms were allowed to relax. This calculation confirms the two Li positions within the oxygen octahedron found experimentally (Figure 2). The corresponding energy barriers between the two sites are 0.26 eV for lithium anatase (model 3) and 0.026 eV for lithium titanate (model 2). In lithium anatase (model 3), the statically calculated separation between the two lithium ions is 1.3 Å and, for lithium titanate (model 2), the distance between site I and II is 0.6 Å, in reasonable agreement with the neutron diffraction result (1.61 Å for lithium anatase and 0.7 Å for lithium titanate). The calculations correctly reproduce the symmetry of the Li positions in anatase with respect to the octahedron center and the distortion of two Li positions in lithium titanate with respect to the center of the oxygen octahedron.

Discussion: Quasi-Elastic Neutron Scattering and Molecular Dynamics. The line broadening in quasi-elastic neutron scattering indicates thermally activated lithium dynamics in lithium titanate with a correlation time of 1.7 ps at 250 K. We distinguish three possible processes on the basis of a difference

in their typical time scales: (1) interoctahedron jumps, (2) intraoctahedron jumps (between site I and II), and (3) local lithium vibrations. Random lithium hopping from one octahedral site to another, approximately separated by 2.5−3.5 Å (see section 3) on a time scale of picoseconds would lead to diffusion, where the lithium is not confined within a specific volume. Hence, this would result in a strong decrease of the EISF with Q and also in a Q dependence of the line width (Q^2 for random diffusion) for the Q range probed, neither of which are observed (conform Figures 6 and 10). This is consistent with our recent NMR experiments,[15] where for Li in lithium titanate the mean residence time between these interoctahedral hops was determined to be on a much longer time scale of around 40 μs at 250 K. Clearly, another faster dynamical process with limited spatial amplitude causes the quasi-elastic signal. To discriminate between the intraoctahedron lithium hopping and local vibrations, the MD simulations were performed. For the ordered lithium "chain" model (model 2), the MD simulations reproduce the distinguishable lithium sites (I and II) in lithium titanate that were determined crystallographically. The MD simulations at 250 K result in a correlation time of femtoseconds up to 0.2 ps for the local vibrations and roughly around 3 ps for the intraoctahedron hops. The latter is in good agreement with the experimental correlation time of 1.7 ps at 250 K. Clearly, the MD correctly predicts the existence of the two available Li ion sites within the oxygen octahedron and the correlation time for the hopping between them in lithium titanate. The local Li ion vibrations with calculated frequencies higher than 5×10^{12} Hz (>0.02 eV) are outside the energy scale probed by the quasi-elastic neutron experiment.

Now that the time scale of the intraoctahedron lithium jumps have been determined, we can look back to one of the questions that prompted this study: the origin of the difference in the homogeneous ^{7}Li MAS NMR line widths in lithium anatase and lithium titanate, the latter being roughly a factor of 5 broader.[15] The inequivalent lithium sites in lithium titanate, Li_I and Li_{II}, might explain the line width in terms of a distribution of chemical and/or quadrupolar shifts. However, the actual ^{7}Li MAS NMR line width (~1 kHz at 9.4 T) is not consistent with the time scale of the intraoctahedron lithium mobility. Li ion mobility on a 1.7 ps time scale will effectively result in a single well-defined averaged ^{7}Li NMR environment (motional averaging). Hence, the two Li ion positions in lithium titanate, site I and II, do not explain the large observed ^{7}Li NMR MAS line width in lithium titanate. We conclude that the line width of the ^{7}Li NMR MAS resonance in lithium titanate is probably related to a weak coupling with the electrons.[17]

The energy barrier calculated (statically) via molecular mechanics for intraoxygen octahedron hops, allowing the lattice to relax, resulted in 0.26 eV for lithium anatase and 0.026 eV in lithium titanate. The latter is significantly larger than the 5.7 meV found experimentally for lithium in lithium titanate. Although no experimental result is available for the barrier in lithium anatase, it is also relatively large if we consider that the experimental value found by NMR for interoctahedron diffusion[15] (which may be expected to be much higher) is 0.2 eV. Similarly, the interoctahedron barrier itself, 0.2 eV in lithium anatase and 0.09 eV in lithium titanate, appears to be overestimated by static calculations performed by other authors, ≥0.5 eV for lithium anatase[13] and 0.5 eV for lithium titanate.[27] Because the calculated "static" barrier height is too high, this implies that the lithium mobility is stimulated by the dynamics of its environment, which is partially taken into account in the MD simulations but totally absent in the molecular mechanics. In performing static energy calculations, one assumes that the time scales of the diffusing particle and that of the environment, the lattice, are uncorrelated. The particle is fixed, and at each step of the diffusion process, the lattice is allowed to relax. However, in reality the diffusive motion is usually stimulated and controlled by coupling with the fluctuations of the environment, leading to lower effective energy barriers.[28] Also coupling between the diffusing particles can lead to reduced barriers for diffusion.[29] In the lithium titanate phase, the suggested Li ion ordering in the a direction might indicate such a coupling.

The time and length scales of the intraoxygen octahedron dynamics are of the order of picoseconds and angstroms. It should be noted that this is on a much shorter time scale than the interoxygen octahedron Li ion diffusion[15] and the interphase domain Li ion diffusion,[16] which are of the order of microseconds and milliseconds, respectively.

5. Concluding Remarks

Inserting lithium into anatase results in phase separation in a lithium-poor phase, composition $Li_{0.026}TiO_2$ with the original anatase structure, and a lithium-rich phase, composition $Li_{0.52}TiO_2$ with a slightly different structure compared with anatase. In both phases, two Li ion positions appear to be available within the oxygen octahedron (see Figure 4).

The finding of discrete Li sites inside distorted oxygen octahedra is, to the best of our knowledge, rather remarkable. However, one would expect that Li intercalated TiO_2 is not the only oxide in which this occurs but that this is much more general for (transition metal) oxides. The fact that such discrete sites have not been observed before is probably related to the difficulty of observing Li in diffraction experiments, or the difficulty in assigning resonances of a local probe like NMR for that matter. In neutron diffraction performed with an inferior resolution, statistics, and less wide d ranges, these sites will simply not be resolved and, in the best cases, will just be identified as an anisotropic temperature factor. Clearly this is not the actual situation. An electron in the material will not interact with the Li at a position described by temperature factors but with the instantaneous Li position that is on either of the multiple sites. The structure also appears less regular because the Li can occupy multiple sites in an octahedron. One of the consequences is that theoretical work on this type of compounds will require modifications; special care should be taken with respect to the Li positions.

The Li positions in anatase are found symmetrically above and below the middle of the surrounding oxygen octahedron (see Figure 4). These positions are reproduced by MD simulations (model 3, Figure 8). The distinguishable Li sites in lithium titanate are reproduced by force field molecular dynamics simulations only if a specific Li ordering is assumed. This ordered structural model can be argued on the basis of simple repulsive Coulomb interactions between the Li ions. However, it does not lead to a superstructure in the neutron diffraction

(27) Koudriachova, M. V.; Harrison, N. M.; Leeuw, S. W. *Phys. Rev. Lett.* **2001**, *86*, 1275−1278.
(28) Rezayi, E. H.; Suhl, H. *Phys. Rev. B* **1982**, *25*, 2324.
(29) Beyeler, H. U.; Pietronero, L.; Strassler, S. *Phys. Rev. B* **1980**, *22*, 2988.

powder patterns because of the short range of the ordering in combination with the slow Li ion hopping between the neighboring octahedra. The simulations thus show that Li−Li interactions are of considerable influence in this system. The temperature dependence of the lithium occupation in site I and II in lithium titanate reveals a 3.4 meV energy difference between the sites. The combination of molecular dynamics simulations and quasi-elastic neutron scattering provides insight into the intraoctahedron dynamics between the two sites. Quasi-elastic neutron scattering reveals a correlation time of about 1.7 ps at 250 K for lithium hopping between the two sites located within the oxygen octahedron. This hopping appears to be thermally activated from which a 5.7 meV potential barrier between the sites can determined. The overestimation of potential barriers by static calculations for lithiated TiO_2 may illustrate the importance of lattice dynamics in the Li ion mobility in this system.

Acknowledgment. This work is a contribution from the Delft Institute for Sustainable Energy (DISE). Financial support from The Netherlands Organization for Scientific Research (NWO) is gratefully acknowledged. We thank M. Hofmann and D. Visser for assistance with the diffraction measurements.

JA028165Q